

**SYNTHESIS AND BIOLOGICAL ACTIVITY OF  
BENZIMIDAZOLE ANALOGS AS SIRTUIN  
ENZYME INHIBITORS**

**YEONG KENG YOON**

**UNIVERSITI SAINS MALAYSIA**

**2016**

**SYNTHESIS AND BIOLOGICAL ACTIVITY OF  
BENZIMIDAZOLE ANALOGS AS SIRTUIN  
ENZYME INHIBITORS**

by

**YEONG KENG YOON**

**Thesis submitted in fulfillment of the requirements**

**for the Degree of**

**Doctor of Philosophy**

**July 2016**

## ACKNOWLEDGEMENTS

First and foremost, I would like to thank deeply my main supervisor Professor Tan Soo Choon for his guidance, dedication and patience over the past four years. His valuable advice and insight concerning matters on and off the project will forever serve as a guiding light to me. I will miss our occasional little chats. I would also like to thank my co-supervisors Professor Rusli Ismail and Dr Oon Chern Ein, for their useful suggestions and their enthusiasm shown towards my doctoral project. I would like to highlight my appreciation to the Higher Education Ministry for partly supporting my studies.

My deep gratitude goes out to Dr. Mohamed Ashraf Ali, for being a dedicated mentor and for introducing such a wonderful branch of science (medicinal chemistry) to me. It is a pleasure to get to know you. I would also like to record my appreciation to the various collaborators of this project, Professor Hasnah Osman (School of Chemical Sciences, USM), Professor Fun and Dr Quah (School of Physical Sciences, USM), Professor Kaykavous Parang (Department of Pharmacy, University of Rhode Island) and the research team in Alwar Pharmacy College India, without whose help this project would not have been successfully completed. Apart from that, I would also like to thank Dr Michael Zheng, Vice President of Romer Labs Singapore and the rest of the Romer Labs Malaysia team for their support all these years. And to those whose names are not mentioned, I thank you all the same.

To my research mates, I want you to know that it has been simply exceptional to get to know you and I must say we had one heck of a time! I wish you all the best in your future undertakings. It was in this research lab that I met my other half and

best friend, Chee Wei. Thank you for coming into my life and touching me with your love and care. Thank you for your support and for always believing in me. For the insightful discussions, the daily phone calls, the constant reminders. Really couldn't thank you enough. Danke danke danke!

Finally, I would like to extend my deepest gratitude to my family, for all they have done for me and for all their sacrifices. Mom and dad, I just want to tell you that you inspired me!

## TABLE OF CONTENTS

<b>ACKNOWLEDGEMENTS</b>	ii	
<b>TABLE OF CONTENTS</b>	iv	
<b>LIST OF TABLES</b>	x	
<b>LIST OF FIGURES</b>	xi	
<b>LIST OF ABBREVIATIONS</b>	xviii	
<b>ABSTRAK</b>	xxiv	
<b>ABSTRACT</b>	xxvi	
<b>CHAPTER 1</b>	<b>INTRODUCTION TO SIRTUIN BIOLOGY</b>	<b>1</b>
1.1	Sirtuins and histone deacetylases	1
1.2	The history of sirtuins	3
1.3	Overview of biochemical and catalytic activities of sirtuins	3
1.4	Roles of sirtuins in cancer	8
1.4.1	SIRT1	9
1.4.2	SIRT2	11
1.4.3	SIRT3	13
1.4.4	SIRT4	15
1.4.5	SIRT5	16
1.4.6	SIRT6	16
1.4.7	SIRT7	17
1.5	Different classes of sirtuin inhibitors	17
1.5.1	Nicotinamide derivatives	18
1.5.2	Suramin and its analogs	19

1.5.3	Splitomycin and its analogs	20
1.5.4	Hydroxynaphthaldehyde derivatives	21
1.5.5	Thiobarbiturates derivatives	24
1.5.6	Indole derivatives	24
1.5.7	Tenovin derivatives	25
1.5.8	Peptidomimetics	26
1.5.9	Other diverse structural cores	27
1.5.10	Benzimidazole derivatives	30
1.6	Aim and objectives of the present project	31
<b>CHAPTER 2</b>	<b>DESIGN, SYNTHESIS AND</b>	<b>32</b>
	<b>CHARACTERIZATION OF COMPOUNDS</b>	
2.1	Introduction	32
2.2	Aim of study	35
2.3	Material	35
2.4	Instrumentation	39
2.5	Method	39
2.5.1	Synthetic procedures	40
2.5.1(a)	Conventional method	40
2.5.1(b)	One-pot method	43
2.6	Results and discussion	45
2.7	Conclusion	65

<b>CHAPTER 3</b>	<b>BENZIMIDAZOLE DERIVATIVES AS</b>	<b>66</b>
	<b>SIRTUININHIBITORS AND EVALUATION OF</b>	
	<b>THEIR GROWTH INHIBITORY ACTIVITIES</b>	
	<b>ON CANCER CELLS</b>	
3.1	Introduction	66
3.2	Aim of study	67
3.3	Material	67
3.4	Instrumentation	69
3.5	Method	69
3.5.1	Measurement of SIRT1 activity using <i>in vitro</i> assay	69
3.5.2	Measurement of SIRT2 activity using <i>in vitro</i> assay	71
3.5.3	Green autofluorescence	72
3.5.4	Cell proliferation assay	73
3.6	Results and discussion	74
3.6.1	Sirtuin inhibitory activities	74
3.6.2	Growth inhibitory activities on cancerous cells	83
3.7	General statement on inhibitors activities	89
<b>CHAPTER 4</b>	<b>CHARACTERIZATION OF THE</b>	<b>91</b>
	<b>BINDING PROPERTIES OF TARGET</b>	
	<b>COMPOUNDS TOWARDS SIRT1 AND SIRT2</b>	
4.1	Introduction	91
4.2	Aim of study	94
4.3	Material	94
4.4	Method	95

4.5	Results and discussion	95
4.5.1	Molecular docking analysis of test compounds against SIRT2	95
4.5.2	Molecular docking analysis of test compounds against SIRT1	104
4.6	Conclusion	106
<b>CHAPTER 5</b>	<b>LEAD COMPOUND 4h: STUDIES OF ITS PHYSICOCHEMICAL PROPERTIES AND EVALUATION OF ITS POTENTIAL AS ANTICANCER AGENT</b>	<b>107</b>
5.1	Introduction	107
5.2	Aim of study	108
5.3	Material	108
5.4	Instrumentation	112
5.5	Method	113
5.5.1	Inhibitor binding mode	113
5.5.2	Co-factor competition analysis	113
5.5.3	Thermal and freeze-thaw stability	114
5.5.4	Aqueous solubility analysis and molar extinction coefficient	114
5.5.5	Quantum yield	115
5.5.6	Fluorescence imaging in cells	116
5.5.7	Preparation of cell lysates for western blot	117
5.5.8	Protein determination assay for western blot	117

5.5.9	Preparation of polyacrylamide gel (12%) for western blot	118
5.5.10	Preparation of buffers for western blot	119
5.5.11	Western blot analysis	120
5.5.12	Cell proliferation assay	122
5.5.13	Clonogenic assay	124
5.6	Results and discussion	125
5.6.1	Stability of lead compound <b>4h</b>	125
5.6.2	Binding mode of lead compound <b>4h</b>	127
5.6.3	Competition analysis of compound <b>4h</b> with co-factor NAD <sup>+</sup>	130
5.6.4	Water solubility of lead compound <b>4h</b>	131
5.6.5	Fluorescence properties	132
5.6.6	Validation of <i>in vitro</i> results through Western Blot	137
5.6.7	Comparison on anti proliferative activities of compound <b>4h</b> with other sirtuin inhibitors in colorectal cancer cells	139
5.6.8	Colony growth of <b>4h</b> -treated colorectal cancer cell lines	146
5.7	Conclusion	148
<b>CHAPTER 6 GENERAL DISCUSSION</b>		<b>149</b>
6.1	Remarks	149
6.2	Future work	154

<b>REFERENCES</b>	<b>155</b>
<b>APPENDIX A</b>	<b>178</b>
<b>APPENDIX B</b>	<b>239</b>
<b>APPENDIX C</b>	<b>249</b>
<b>APPENDIX D</b>	<b>255</b>
<b>LIST OF PUBLICATIONS</b>	<b>257</b>
<b>LIST OF PATENTS</b>	<b>258</b>

## LIST OF TABLES

		Page
Table 1.1	Some downstream targets of SIRT1-7.	8
Table 2.1	Structure of Series 1 to Series 6 compounds with substitution at <b>R</b> <sup>1</sup> and <b>R</b> <sup>2</sup> positions.	46
Table 2.2	<sup>1</sup> H NMR assignments for hydrogens of the side chain at the <b>R</b> <sup>1</sup> position	60
Table 2.3	N-Alkylation of intermediate <b>I</b> with different amines.	63
Table 2.4	Comparison of the conventional 4-step synthetic method with the novel one-pot green synthetic method.	64
Table 3.1	SIRT1 and SIRT2 inhibitory activities of synthesized benzimidazole derivatives.	76
Table 4.1	Residues within 5 Å of the NAD <sup>+</sup> co-factor and acetyl lysine channel binding pockets.	98
Table 5.1	Absorbance of compound <b>4h</b> measured from Week 0 - Week 4 at 25°C ( $\lambda_{ex} = 346$ nm). Percentage of degradation was calculated relative to Week 0 (time where compound <b>4h</b> was freshly prepared).	126
Table 5.2	Absorbance of compound <b>4h</b> measured through 10 freeze-thaw cycles ( $\lambda_{ex} = 346$ nm). Percentage of degradation was calculated relative to Cycle 0 (time where compound <b>4h</b> was freshly prepared).	127
Table 5.3	The effect of compound <b>4h</b> on the colorectal cancer cell growth inhibition after 24, 48 and 72 hours treatment.	140
Table 5.4	IC <sub>50</sub> values of compound <b>4h</b> , 5-fluorouracil and other well-established sirtuin inhibitors against HCT116, HT29, LIM1215 and Caco-2 cell lines.	143
Table 5.5	Selectivity index comparison between compound <b>4h</b> and Tenovin-6.	145
Table C1	Growth inhibitory activities for the synthesized compounds (Series 1-Series 6) on CCRF-CEM, HCT-116 and MDA-MB-468 cell lines at 50 $\mu$ M.	249

## LIST OF FIGURES

	<b>Page</b>
Figure 1.1	2
Enzymatic reactions catalyzed by sirtuin enzymes. In addition to the deacetylation of lysine residues (A), other reaction mechanisms such as lysine demalonylation, desuccinylation, deglutarylation (B), and mono-ADP-ribosylation (C) have been reported. The members of the sirtuin family catalyzing the various reactions are given on the arrows.	
Figure 1.2	4
Schematic representation of SIRT1-7. Each sirtuin is characterized by an approximately conserved 275 amino acid catalytic core (in yellow) with unique additional N-terminal and/or C-terminal sequences of variable length (in blue).	
Figure 1.3	5
Cellular localization and enzymatic activities of the mammalian sirtuins. SIRT1 is predominantly expressed in the nucleus and the cytoplasm. SIRT2 is mainly expressed in the cytoplasm but may be shuttled to the nucleus during mitosis. SIRT3, SIRT4 and SIRT5 are mainly localized in the mitochondria. SIRT6 and SIRT7 are confined to the nucleus. SIRT1, SIRT2 and SIRT3 possess deacetylase activity whereas SIRT4 modulates ADP-ribosylation activity. Apart from deacetylase activity, SIRT5 possess demalonylase and desuccinylase activities while SIRT6 possess ADP-ribosyltransferase, demyristoylase and depalmitoylase actions.	
Figure1.4	13
Dual role of sirtuin in cancer. Below the stress threshold, sirtuin promotes DNA repair and ultimately cell survival. Above chronic stress threshold, sirtuin induces tumor formation and cancer.	
Figure 1.5	19
Structure of nicotinamide.	
Figure 1.6	20
Structure of Suramin and NF675.	
Figure 1.7	21
Structure of Splitomicin and HR73.	
Figure 1.8	22
Structure of Sirtinol and Slermide.	
Figure 1.9	23
Structure of cambinol and other sirtuin inhibitors with the hydroxynaphthaldehyde moiety.	

Figure 1.10	Structure of EX-527.	25
Figure 1.11	Structure of Tenovin-1 and Tenovin-6.	26
Figure 1.12	Structure of some peptidomimetic sirtuin inhibitors.	27
Figure 1.13	Structure of AGK2 and Ro31-8220.	29
Figure 1.14	Structure of indole and benzimidazole.	30
Figure 1.15	Flowchart of studies for this project.	31
Figure 2.1	Structure of benzimidazole and its numbering system.	32
Figure 2.2	Early scheme used by Hoebrecker to synthesize benzimidazoles (Hoebrecker, 1872).	32
Figure 2.3	Scheme used by Ladenburg to produce benzimidazoles (Ladenburg, 1875).	33
Figure 2.4	Some widely used drugs which contain the benzimidazole moiety.	33
Figure 2.5	The conventional synthetic scheme for the targeted compounds (1,2-disubstituted benzimidazoles).	41
Figure 2.6	New protocol developed to synthesize target compounds.	44
Figure 2.7	<sup>1</sup> H NMR assignment for representative compound <b>4h</b> .	55
Figure 2.8	<sup>1</sup> H NMR spectrum of compound <b>4h</b> in CDCl <sub>3</sub> (500 MHz).	56
Figure 2.9	<sup>13</sup> C NMR spectrum of compound <b>4h</b> in CDCl <sub>3</sub> (500 MHz).	58
Figure 2.10	Hydrogen bond driven formation of the Meisenheimer adduct ( <b>I-II</b> complex) in facilitating N-alkylation. Dashed lines represent hydrogen bonds.	62
Figure 2.11	Synthetic protocols which were utilized to generate the interested benzimidazole analogs. The one-pot method proved advantageous in many ways compared to the conventional method.	65

Figure 3.1	Schematic diagram of steps involved in the sirtuin <i>in vitro</i> enzymatic assay (Modified from Yarlagadda, Cruz Jr., Sun, Zhong, Wang, & Rakhmanova, retrieved July 2015).	75
Figure 3.2	Bar chart showing Series 4 having more active compounds compared to other series.	80
Figure 3.3	Bar chart showing Series 4 having more active compounds compared to other series.	81
Figure 3.4	Compound <b>4h</b> with its SIRT1/2 IC <sub>50</sub> values.	83
Figure 3.5	Cell viability effects of CCRF-CEM, HCT116 and MDA-MB-468 cancer cells after treatment with compounds from Series 1-3 at 50 µM. Experiments were done in triplicates (n=3). Error bar refers to standard deviation (S.D.).	85
Figure 3.6	Cell viability effects of CCRF-CEM, HCT116 and MDA-MB-468 cancer cells after treatment with compounds from Series 4-6 at 50 µM. Experiments were done in triplicates (n=3). Error bar refers to standard deviation (S.D.).	86
Figure 3.7	Color-coded grid showing the most potent compounds (in blue) which are active against at least 2 out of 3 tested cancer cell lines.	87
Figure 3.8	Red squares indicate potent sirtuin inhibitors which possessed good antiproliferative activities. Potent sirtuin inhibitors with weak antiproliferative activities are coloured yellow while compounds with good growth inhibitory effect but are not potent sirtuin inhibitors are coloured blue.	88
Figure 3.9	Sirtuin inhibitory activities shown by the synthesized benzimidazole analogs are correlated to cancer cell growth.	90
Figure 4.1	Crystal structure of apo-SIRT2 to represents the illustration of the overall structure of the sirtuin enzyme (Modified from Moniot, Schutkowski, & Steegborn, 2013).	92
Figure 4.2	Current molecular docking approaches.	93
Figure 4.3	Control dock showing ADPr molecule (blue) docked in human SIRT2 (PDB: 3ZGV).	96

Figure 4.4	Magnified diagram focusing on amino acids within 10 Å of the ADPr molecule. The 3 subdomains of the co-factor binding site (A-, B-, and C-pocket) as well as the acetyl lysine channel, which is the substrate binding site, are highlighted.	97
Figure 4.5	(A) Compound <b>4h</b> (green) docked into the active site of SIRT2. It was postulated to compete with NAD <sup>+</sup> as it was found to overlap nicely with ADPr (blue); (B) Close-up of the overlap between <b>4h</b> and ADPr ligand. (PDB: 3ZGV).	99
Figure 4.6	Molecular interactions between <b>4h</b> and SIRT2. Molecular interactions observed between <b>4h</b> and SIRT2 (within 5 Å). Important interactions include those with Ser263, Thr262, Gln167, Arg97, His187 and Phe96. (PDB code: 3ZGV).	99
Figure 4.7	Strong hydrogen bond interactions between imidazole moiety of compound <b>4h</b> with Ser263 and Thr262. (PDB code: 3ZGV).	100
Figure 4.8	Hydrogen bond interactions between compound <b>4h</b> and (A) residue Gln167 and (B) residue Arg97. (PDB code: 3ZGV).	101
Figure 4.9	Compound <b>4h</b> (green), <b>4d</b> (red) and <b>4e</b> (yellow) were docked into the active site of SIRT2 (PDB code: 3ZGV). It showed that compound <b>4h</b> were optimally fitted into the ADPr binding site (blue) while the phenolic substituent of <b>4d</b> and the anisole substituent of <b>4e</b> were shifted out from the ADPr binding site. This resulted in less favourable complexes and weaker SIRT2 inhibitory activities for <b>4d</b> and <b>4e</b> .	102
Figure 4.10	Overlay of the six compounds from Series 1-6 with piperidinyl substituent at R <sup>1</sup> . Compound <b>1h</b> (magenta), <b>2h</b> (cyan), <b>3h</b> (yellow) and <b>5h</b> (marine blue) were shown to have different orientation as compound <b>4h</b> (green) and <b>6h</b> (orange) when docked in the cavity of SIRT2 (PDB code: 3ZGV).	103
Figure 4.11	Residues forming the narrow gorge (in yellow) which proved critical in discriminating the orientation and docking location in SIRT2 (PDB code: 3ZGV).	104
Figure 4.12	Overlay of compound <b>4e</b> (brown) and <b>4h</b> (green) when docked in the cavity of SIRT1 (PDB code: 4I5I).	105
Figure 5.1	Compound <b>4h</b> was found to have maximum absorption, $\lambda_{\max}$ at 346 nm.	126

Figure 5.2	Plots of product formation versus time in the absence and presence of 10 $\mu\text{M}$ of <b>4h</b> for (A) SIRT1 and (B) SIRT2. AFU stands for arbitrary fluorescence unit.	128
Figure 5.3	Kinetic scheme for reversible enzyme inhibitors.	129
Figure 5.4	Kinetic scheme for irreversible enzyme inhibitors.	129
Figure 5.5	Decreasing SIRT2 inhibition by compound <b>4h</b> with increasing concentrations (100, 200, 333, 500 and 1000 $\mu\text{M}$ ) of $\text{NAD}^+$ .	131
Figure 5.6	Plot of absorbance versus concentration of compound <b>4h</b> in DMSO. The graph was used to calculate the water solubility of <b>4h</b> . The concentration can be determined when the absorbance is known.	132
Figure 5.7	Compound <b>4h</b> was found to have fluorescence attribute with $\lambda_{\text{em}}$ at 448 nm when light-irradiated at $\lambda_{\text{ex}} = 346$ nm.	133
Figure 5.8	Fluorescent images of compound <b>4h</b> at different concentrations (0.5 - 50 $\mu\text{M}$ ) in DMSO.	134
Figure 5.9	Quantum yield ( $\phi$ ) of compound <b>4h</b> in DMSO (red) and in 0.01 M PBS (blue). Quinine sulphate was used as reference (green). AFU stands for arbitrary fluorescence unit.	135
Figure 5.10	Fluorescence microscopy images of compound <b>4h</b> in cells. Live-cell images of HCT116 cells (A – bright-field, F - fluorescence), HT29 cells (B – bright-field, G - fluorescence), LIM1215 cells (C – bright-field, H - fluorescence), Caco-2 cells (D – bright-field, I - fluorescence) and CCD-18co colon fibroblast (E – bright-field, J - fluorescence) incubated with <b>4h</b> . Arrows point to cell nucleus. Bar represents 100 $\mu\text{m}$ .	136
Figure 5.11	Effects of sirtuin inhibitors on alpha-tubulin (A) and p53 (B) acetylation. Control (1); 10 $\mu\text{M}$ EX-527 (2); 10 $\mu\text{M}$ AGK2 (3); 10 $\mu\text{M}$ <b>4h</b> (4); 50 $\mu\text{M}$ <b>4h</b> (5).	138
Figure 5.12	Effects of sirtuin inhibitors on acetyl p53 after adding 1 $\mu\text{M}$ of etoposide in the treatment. Control (1); 10 $\mu\text{M}$ EX-527 (2); 10 $\mu\text{M}$ AGK2 (3); 10 $\mu\text{M}$ <b>4h</b> (4); 50 $\mu\text{M}$ <b>4h</b> (5).	139

Figure 5.13	Representative plot of cell growth inhibition (%) versus concentration ( $\mu\text{M}$ ) of compound <b>4h</b> on (A) HCT116, (B) HT29, (C) LIM1215 and (D) Caco-2. Half maximal inhibitory concentration ( $\text{IC}_{50}$ ) values were determined from these curves.	141
Figure 5.14	Snapshots showing the changes in cell morphology. (A) HCT116 cell before treatment, (B) after treatment with 50 $\mu\text{M}$ <b>4h</b> ; (C) HT29 cell before treatment, (D) after treatment with 50 $\mu\text{M}$ <b>4h</b> ; (E) LIM1215 cell before treatment, (F) after treatment with 50 $\mu\text{M}$ <b>4h</b> ; (G) Caco-2 cell before treatment, (H) after treatment with 50 $\mu\text{M}$ <b>4h</b> .	142
Figure 5.15	Clonogenic assay showing (A) HCT116, (B) HT29 and (C) LIM1215 growth patterns after treatment with compound <b>4h</b> . 5-FU was used as positive control.	147
Figure 6.1	Key SAR findings for the sirtuin inhibitory activity and growth inhibitory effect of newly synthesized benzimidazoles.	150
Figure A1	$^1\text{H}$ NMR spectrum of compound <b>1f</b> .	233
Figure A2	$^1\text{H}$ NMR spectrum of compound <b>2f</b> .	234
Figure A3	$^1\text{H}$ NMR spectrum of compound <b>3f</b> .	235
Figure A4	$^1\text{H}$ NMR spectrum of compound <b>4f</b> .	236
Figure A5	$^1\text{H}$ NMR spectrum of compound <b>5f</b> .	237
Figure A6	$^1\text{H}$ NMR spectrum of compound <b>6f</b> .	238
Figure B1	Crystal structure of compound <b>1i</b> . The dashed line indicates a hydrogen bond.	239
Figure B2	Crystal structure of compound <b>1o</b> .	240
Figure B3	Crystal structure of compound <b>2l</b> .	240
Figure B4	Crystal structure of compound <b>2m</b> .	241
Figure B5	Crystal structure of compound <b>3a</b> .	241

Figure B6	Crystal structure of compound <b>3e</b> .	242
Figure B7	Crystal structure of compound <b>3i</b> . The dashed line indicates a hydrogen bond.	242
Figure B8	Crystal structure of compound <b>3k</b> .	243
Figure B9	Crystal structure of compound <b>3n</b> .	243
Figure B10	Crystal structure of compound <b>3o</b> .	244
Figure B11	Crystal structure of compound <b>4e</b> .	244
Figure B12	Crystal structure of compound <b>5f</b> .	245
Figure B13	Crystal structure of compound <b>5l</b> .	245
Figure B14	Crystal structure of compound <b>5m</b> .	246
Figure B15	Crystal structure of compound <b>5n</b> . The dashed line indicates a hydrogen bond.	246
Figure B16	Crystal structure of compound <b>5o</b> .	247
Figure B17	Crystal structure of compound <b>6a</b> .	247
Figure B18	Crystal structure of compound <b>6i</b> .	248
Figure D1	UV spectra of <b>4h</b> (10 $\mu$ M) superimposed when freshly prepared (A) and showing decreased absorbance as a function of incubation at 25°C (B).	255
Figure D2	UV spectra of <b>4h</b> (10 $\mu$ M) superimposed when freshly prepared (A) and showing decreased absorbance as a function of freeze-thaw cycle (B).	255
Figure D3	UV spectra of <b>4h</b> in decreased concentration from 20 $\mu$ g/mL (A) to 0.25 $\mu$ g/mL (B) in DMSO. Water solubility and molar extinction coefficient of <b>4h</b> are determined from this plot.	256

## LIST OF ABBREVIATIONS

%	Percent
°C	Degree Celsius
Å	Angstrom
δ	Delta, chemical shift scale
μL	Microliter
μM	Micromolar
λ <sub>max</sub>	Wavelength of maximum absorption
λ <sub>ex</sub>	Wavelength of maximum excitation
λ <sub>em</sub>	Wavelength of maximum emission
α	Alpha
β	Beta
ACS	Acetyl-CoA-synthetase
ADP	Adenosine diphosphate
ADPr	Adenosine diphosphate ribose
AFU	Arbitrary fluorescence unit
Ala	Alanine
Arg	Arginine
Asn	Asparagine
Asp	Aspartic acid
ATCC	American Type Culture Collection
BCL	B-cell lymphoma
Br	Bromine
BRCA	Breast cancer gene

$^{13}\text{C}$ NMR	Carbon nuclear magnetic resonance
$\text{CDCl}_3$	Deuterated chloroform
CDH	Cadherin
$\text{CF}_3$	Trifluoromethyl
$\text{CH}_3$	Methyl
CHN	Carbon, hydrogen, nitrogen
Cl	Chlorine
COOH	Carboxylic acid
COX	Cytochrome c oxidase
CPS1	Carbamoyl-Phosphate Synthase
CRC	Colorectal cancer
Cys	Cysteine
d	Doublet
dd	Doublet of doublet
DMEM	Dulbecco's modified Eagle's medium
DMSO	Dimethyl sulfoxide
DNA	Deoxyribonucleic acid
DOX	Doxorubicin
EMT	Epithelial-mesenchymal-transition
FBS	Foetal bovine serum
FOXO	Forkhead box protein O
Gln	Glutamine
Glu	Glutamic acid
GLUD	Glutamate dehydrogenase
Gly	Glycine

$^1\text{H}$ NMR	Proton nuclear magnetic resonance
HAT	Histone acetyl-transferase
HCC	Hepatocellular carcinoma
HCl	Hydrochloric acid
HDAC	Histone deacetylase
HIF	Hypoxia-inducible factor
His	Histamine
HMGCS2	Hydroxymethylglutaryl-CoA-synthase 2
IC <sub>50</sub>	Half maximal (50%) inhibitory concentration
Ile	Isoleucine
<i>J</i>	Coupling constant
K-RAS	Kirsten rat sarcoma
LCAD	Long-chain acyl-CoA-dehydrogenase
Lys	Lysine
m	Multiplet
Mar	Mating-type regulator
MEF	Mouse embryo fibroblast
min	Minute
mir	microRNA
mL	Milliliter
mM	Millimolar
MMP	Matrix metalloproteinase
mTORC	Mechanistic Target Of Rapamycin Complex
MTS	3-(4,5-dimethylthiazol-2-yl)-5-(3-carboxymethoxyphenyl)-2-(4-sulfophenyl)-2H-tetrazolium

MYC	myelocytomatosis
$m/z$	Mass-to-charge ratio
N(Et) <sub>2</sub>	Diethylamino
N(CH <sub>3</sub> ) <sub>2</sub>	Dimethylamino
NAD <sup>+</sup>	Nicotinamide adenine dinucleotide
NaOH	Sodium hydroxide
N.D.	Not determined
NF- $\kappa$ B	Nuclear factor kappa B
NMR	Nuclear magnetic resonance
NO <sub>2</sub>	Nitro
Nrf2	Nuclear factor erythroid 2-related factor
OCF <sub>3</sub>	Trifluoromethoxyl
OCH <sub>3</sub>	Methoxyl
OH	Hydroxyl
ORTEP	Oak Ridge thermal ellipsoid plot
OSCC	Oral squamous cell carcinoma
PDB	Protein data bank
PGK	Phosphoglycerate kinase
Phe	Phenylalanine
PPAR	Peroxisome proliferator-activated receptor
ppm	Parts per million
q	Quadruplet
RMSD	Root-mean-square deviation
RNA	Ribonucleic acid
ROS	Reactive oxygen species

RPMI	Roswell Park Memorial Institute
s	Singlet
SAR	Structure-activity relationship
Ser	Serine
SFRP	Secreted frizzled-related protein
SI	Selectivity index
SIR	Silent information regulator
SIRT1	Sirtuin 1
SIRT2	Sirtuin 2
SIRT3	Sirtuin 3
SIRT4	Sirtuin 4
SIRT5	Sirtuin 5
SIRT6	Sirtuin 6
SIRT7	Sirtuin 7
Skp	Seventeen kilodalton proetin
t	Triplet
<i>t</i>	Tertiary
Thr	Threonine
Tyr	Tyrosine
TLC	Thin layer chromatography
TSC	Tuberous sclerosis complex
TMS	Tetramethylsilane
UV	Ultraviolet
UV-Vis	Ultraviolet-Visible
Val	Valine

VEGF	Vascular Endothelial Growth Factor
WHO	World Health Organization
XRD	X-ray diffraction

**SINTESIS DAN AKTIVITI BIOLOGI ANALOG**  
**BENZIMIDAZOLSEBAGAIPERENCAT ENZIM SIRTUIN**

**ABSTRAK**

Bagi mencari perencat enzim sirtuin yang poten, 90 analog benzimidazol telah berjaya direka. Kaedah sintesis yang digunakan dalam projek ini mengambil kira langkah-langkah yang lestari. Sebatian **4h** (ethyl 2-(4-(piperidin-1-yl)phenyl)-1H-benzo[d]imidazole-5-carboxylate) merupakan perencat enzim sirtuin yang paling baik dalam projek ini. Ia didapati merencat sirtuin-2 (SIRT2) lebih baik daripada sirtuin-1 (SIRT1). Daripada profil sebatian dengan aktiviti perencatan SIRT1/SIRT2, perhubungan struktur dengan aktiviti boleh disimpulkan. Juga menarik perhatian ialah kemampuan sebatian **4h** untuk mengekang pertumbuhan sel kanser kolorektal. Selain daripada itu, ia juga mempunyai keupayaan untuk mencegah pertumbuhan sel kanser leukemia dan payudara. Pemodelan komputer turut digunakan untuk memberi penjelasan yang wajar terhadap keputusan aktiviti yang diperolehi. Sebatian **4h** didapati boleh didokkan kedalam tapak aktif enzim SIRT2 dengan menggunakan struktur kristal (PDB: 3ZGV). Walau bagaimanapun, usaha untuk merasionalkan data aktiviti untuk SIRT1 tidak berjaya dilakukan dengan kaedah pemodelan komputer. Beberapa sifat-sifat kimia sebatian **4h** seperti kelarutan dalam air, kestabilan dan pendarfluor sebatian juga dikaji dengan teliti. Berdasarkan kajian literatur, sebatian **4h** merupakan perencat sirtuin pertama yang dilaporkan mempunyai sifat berendarfluor. Ia merupakan kelebihan tambahan kerana boleh digunakan bagi memantau perubahan morfologi serta fenotip sel kanser. Keputusan yang dilaporkan dalam projek ini dengan jelasnya menunjukkan perhubungan antara

perencanaan aktiviti sirtuin dengan kanser apabila 66.7% daripada sebatian yang aktif mempunyai aktiviti anti-kanser yang memberangsangkan. Inijuga membuktikan enzim sirtuin adalah sasaran analog benzimidazol yang dikaji. Sebatian yang mempunyai aktiviti perencanaan sirtuin yang baik serta menunjukkan kesan sitotoksik seperti sebatian **4h** merupakan calon utama pengubahsuaian demi meningkatkan aktiviti dan profil “drug-like” kerana penerokaan benzimidazol mungkin menghasilkan sebatian yang berguna dalam perawatan kanser. Walaupun penyelidikan yang lebih komprehensif masih diperlukan untuk mengetahui dengan lebih mendalam peranan enzim sirtuin terhadap kanser, perencanaan enzim sirtuin merupakan strategi yang baru dan berdaya maju dalam terapi kanser.

# SYNTHESIS AND BIOLOGICAL ACTIVITY OF BENZIMIDAZOLE ANALOGS AS SIRTUIN ENZYME INHIBITORS

## ABSTRACT

In the effort to search for potent sirtuin inhibitors, 90 benzimidazole analogs across 6 series were designed, synthesized and characterized. Compound **4h** (ethyl 2-(4-(piperidin-1-yl)phenyl)-1H-benzo[d]imidazole-5-carboxylate) was identified to be the most potent sirtuin inhibitor in this project with a preference for sirtuin-2 (SIRT2) inhibition over SIRT1. Based on the profile of the compounds along with their demonstrated SIRT1/SIRT2 inhibitory activities, a structure-activity-relationship was deduced for the benzimidazole moiety. Remarkably, compound **4h** exhibited potent growth inhibitory effect on colorectal cancer cell lines. Apart from colorectal cancer, it was also found to possess antiproliferative activity against leukemia and breast cancer cell lines. Molecular docking approach was used to rationalize the observed activity. The SIRT2 crystal homology model (PDB: 3ZGV) was found to be able to accommodate compound **4h** in its active site, thus supporting the notion that **4h** was indeed able to strongly inhibit the SIRT2 activity. However, the structure activity relationship of the compounds towards observed SIRT1 inhibition was unable to be completely rationalized using similar method. In light of the potential of compound **4h** in combating cancer, some relevant physicochemical attributes of **4h** such as water solubility, compound stability and fluorescent properties were determined. Based on literature review, compound **4h** is the first highly fluorescent sirtuin inhibitor reported so far. This is an added advantage as it could be useful in monitoring morphological as well as phenotype changes in cancer cells. In summary,

the results reported in this thesis clearly demonstrated a significant correlation between sirtuin inhibition and cancer as 66.7% of the synthesized compounds with potent sirtuin inhibitory activity possessed antiproliferative effect against cancer cells. Furthermore, it provided a proof of concept that sirtuin enzymes are indeed targets of benzimidazole derivatives. Compounds with potent sirtuin inhibition and which demonstrated cytotoxic effect such as **4h** are prime candidates for further modifications to enhance the activity and drug-like profiles as exploration of the benzimidazole scaffold may eventually yield useful compounds in cancer treatment. Although more research is needed to further elucidate the role of sirtuins in cancer, sirtuin inhibition remains a new and viable strategy in cancer therapy.

# CHAPTER ONE

## INTRODUCTION TO SIRTUIN BIOLOGY

### 1.1 Sirtuins and histone deacetylases (HDACs)

Histone acetyl-transferases (HATs) are enzymes which add acetyl groups to lysine from histones while histone deacetylases (HDACs) remove the acetyl groups. Both HATs and HDACs play important roles in gene expression by regulating the acetylation and deacetylation of histones respectively (Simmons, 2008; Philips & Shaw, 2008).

In general, HATs act as transcriptional gene activators as acetylation of lysine neutralizes the positive charge normally present and subsequently promotes a more relaxed chromatin structure by reducing affinity between histone and the negatively charged DNA. This indirectly renders DNA more accessible to transcription factors (Marks & Xu, 2009). On the contrary, HDACs promote a more condensed chromatin structure and act as transcriptional gene suppressor (Johnstone, 2002). Histone deacetylation represses gene transcription by increasing ionic interactions between the positively charged histones and negatively charged DNA, thus limiting its access to transcription factors.

In humans, 18 HDAC enzymes have been identified, which can be subdivided into four classes (HDAC Class I-IV) primarily based on their homology to yeast HDACs (Blander & Guarante, 2004; Bhalla, 2005). Among these, class I, II and IV HDACs are dependent on  $Zn^{2+}$  for their deacetylase activity. The only exception is class III HDAC, or sirtuins, as they require  $NAD^+$  instead of  $Zn^{2+}$  as a

cofactor (North & Verdin, 2004; Michan & Sinclair, 2007). The role of  $\text{NAD}^+$  in the deacetylase activity of the Silent Information Regulator (SIR2)-like protein was first described in detail by Landry, Slama, and Sternglanz (2000). Then ADP-ribosyl transferase activity of sirtuins was considered a low efficiency side-reaction due to the partial decoupling of intrinsic deacetylation and acetate transfer to ADP-ribose. (Denu, 2005). More recently, mono-ADP-ribosyl transferase activity was found to be the main enzymatic activity of human Sirtuin-4 (SIRT4) and also human Sirtuin-6 (SIRT6) (Liszt, Ford, Kurtev, & Guarante, 2005; Haigis et al., 2006). In general, the enzyme reactions that are catalyzed by sirtuins are depicted in Figure 1.1.

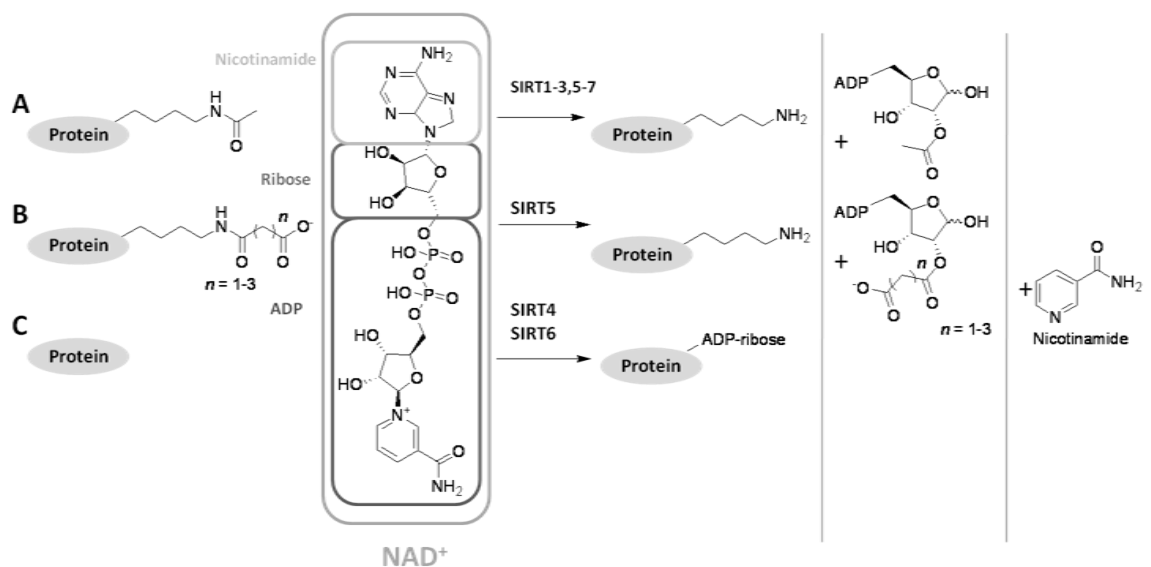


Figure 1.1 Enzymatic reactions catalyzed by sirtuin enzymes. In addition to the deacetylation of lysine residues (A), other reaction mechanisms such as lysine demalonylation, desuccinylation, deglutarylation (B), and mono-ADP-ribosylation (C) have been reported. The members of the sirtuin family catalyzing the various reactions are given on the arrows.

## **1.2 The history of sirtuin**

The class III histone deacetylases (HDACs), or sirtuins include a group of proteins that are homologous with the yeast SIR2 family of proteins. Originally known as Mating-type regulator 1 (Mar1), SIR2 was discovered by Klar et al. in 1979 through spontaneous mutation of the mating-type loci Hidden MAT Right (HMR) and Hidden MAT Left (HML) (Klar, Seymour & Macleod, 1979). SIR2 was later demonstrated to play a major role in silencing genes near telomeres. The silent regions at the telomeres and mating-type loci were later shown to be associated with histones that were hypoacetylated at the  $\epsilon$ -amino group of N-terminal lysine residues (Braunstein, Rose, Holmes, Allis, & Broach, 1993). In 1999, Roy Fyfe had identified and characterized five of the human SIR2 homologues (SIRT1-5) and called the genes “sirtuin” (Fyfe, 1999). In 2000, another two SIR2 homologues (SIRT6 and SIRT7) were added to the family (Fyfe, 2000), making it a total of seven sirtuins having been identified in human (SIRT1-7).

## **1.3 Overview of biochemical and catalytic activities of sirtuins**

Each sirtuin is characterized by an approximately conserved 275 amino acid catalytic core with unique additional N-terminal and/or C-terminal sequences of variable length (Figure 1.2) (Fyfe, 2000).

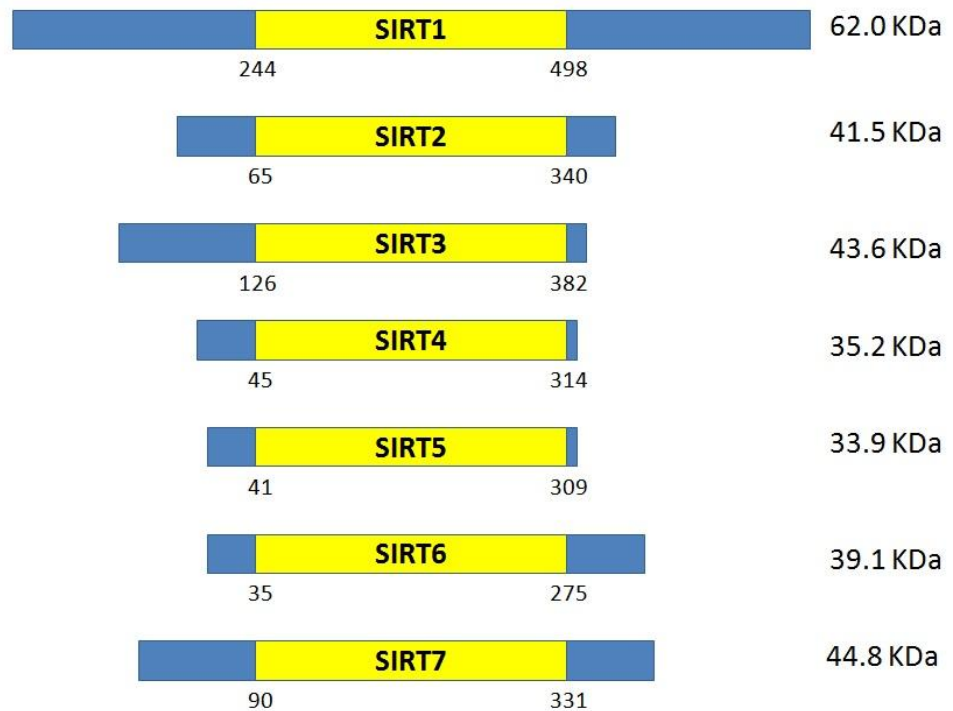


Figure 1.2 Schematic representation of SIRT1-7. Each sirtuin is characterized by an approximately conserved 275 amino acid catalytic core (in yellow) with unique additional N-terminal and/or C-terminal sequences of variable length (in blue).

The side chains are important as they are perceived to serve as “switches” for sirtuin activity. This is because the additional variable N- or C-terminal sequences flanking the catalytic core have been reported to enhance the activity by up to 45-fold (Pan, Yuan, Brent, Ding, & Marmorstein, 2012) and lead to diverse subcellular localizations that contribute to the difference in biological functions (Figure 1.3).

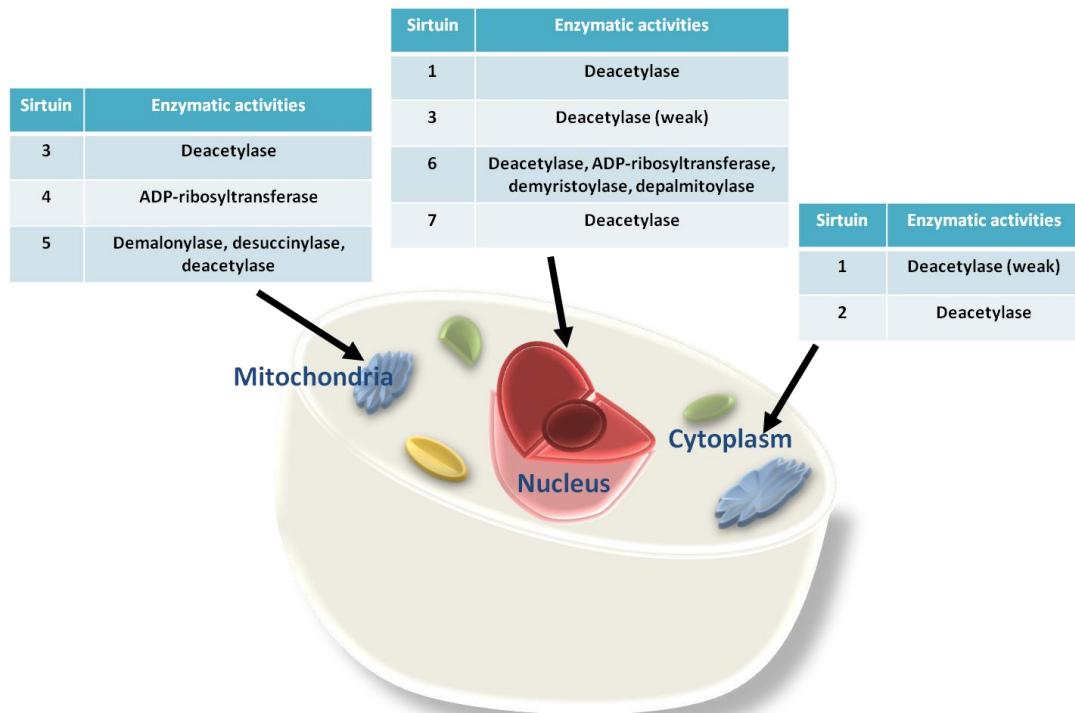


Figure 1.3 Cellular localization and enzymatic activities of the mammalian sirtuins. SIRT1 is predominantly expressed in the nucleus and the cytoplasm. SIRT2 is mainly expressed in the cytoplasm but may be shuttled to the nucleus during mitosis. SIRT3, SIRT4 and SIRT5 are mainly localized in the mitochondria. SIRT6 and SIRT7 are confined to the nucleus. SIRT1, SIRT2 and SIRT3 possess deacetylase activity whereas SIRT4 modulates ADP-ribosylation activity. Apart from deacetylase activity, SIRT5 possess demalonylase and desuccinylase activities while SIRT6 possess ADP-ribosyltransferase, demyristoylase and depalmitoylase actions.

Sirtuin-1 (SIRT1) is the direct homologue of the yeast SIR2 and is mainly located in the nucleus. It has a wide range of cellular functions such as modulating cell survival and regulating the transcriptional activities of NF- $\kappa$ B (Kauppinen, Suuronen, Ojala, Kaamiranta, Salminen, 2013), p53 (Luo, Su, Chen, Shiloh, & Gu, 2000) and FOXO proteins (Berdichevsky & Guarante, 2006). Sirtuin-2 (SIRT2) resides mainly in the cytoplasm. SIRT2 has been shown to deacetylate a number of substrates *in vitro*, including  $\alpha$ -tubulin (Dryden, Nahhas, Nowak, Goustin, & Tainsky, 2003; North, Marshall, Borra, Denu, & Verdin, 2003).

Sirtuin-3 (SIRT3) was the first sirtuin found to be localized in the mitochondria of mammalian cells (Onyango, Celic, McCaffery, Boeke, & Feinberg, 2002). Although many studies have argued for an exclusively mitochondrial function of SIRT3 (Onyango et al., 2002; Schwer, North, Fyre, Ott, & Verdin, 2002), some reports have shown that SIRT3 shuttles to the nucleus (Scher, Vaquero, & Reinberg, 2007; Iwahara, Bonasio, Narendra, & Reinberg, 2012). SIRT3 regulates the acetylation activity of metabolic enzymes such as acetyl-CoA-synthetase (ACS) (Hallows, Lee, & Denu, 2006). Another target of SIRT3, hydroxymethylglutaryl CoA synthase 2 (HMGCS2) regulates ketone body production, thus helping to supply energy to the brain during fasting (Shimazu et al., 2010). Another study by the same group of researchers also revealed a new function of SIRT3 in fatty acid oxidation (Hirschey et al., 2010). It was shown that SIRT3 deacetylates long-chain acyl CoA dehydrogenase (LCAD) and upregulates its enzymatic activity during fasting. In short, SIRT3 may be especially important under energy limitation conditions.

Sirtuin-4 (SIRT4) is a mitochondrial sirtuin which is involved in metabolism. In contrast to SIRT3, SIRT4 has not been reported to possess deacetylation activity but only ADP-ribosylation activity (Haigis et al., 2006). It has been shown that SIRT4 can repress glutamate dehydrogenase in pancreatic  $\beta$ -cells and control the insulin secretion (Haigis et al., 2006). Interestingly, although SIRT3 and SIRT4 both play an important role in metabolic regulation, they have opposing roles in glutamate dehydrogenase regulation and fatty acid oxidation (Nasrin et al., 2010).

Localized in mitochondria, Sirtuin-5 (SIRT5) has weak deacetylase activity but does not appear to possess ADP-ribosyltransferase activity (Haigis et al., 2006). SIRT5 was originally reported to deacetylate carbamoyl-phosphate synthase 1 (CPS1) and play a role in the regulation of urea cycle (Nakagawa, Lomb, Haigis, & Guarante, 2009). However, the demalonylation and desuccinylation actions of SIRT5 on CPS1 and other proteins are now thought to be more prominent than its deacetylation activities (Du et al., 2011).

Like SIRT1, Sirtuin-6 (SIRT6) is abundant in the nucleus. Biochemically, SIRT6 has been shown to demonstrate robust ADP-ribosyltransferase activity but only weak deacetylase activity (Liszt et al., 2005; Michishita et al., 2009). Pan and colleagues have shown that its deacetylation rate was approximately 1000 times weaker compared to other highly active sirtuins (Pan et al., 2011). Recently, SIRT6 was shown to also possess demyristoylase and depalmitoylase activities (Jiang et al., 2013). Similar to SIRT1, SIRT6 is a transcriptional regulator. Hence deficiency in SIRT6 may alter the expression of many downstream genes (Kawahara et al., 2011; Tennen & Chua, 2011). Some of SIRT6's target genes include nuclear factor-kappaB (NF- $\kappa$ B) as well as hypoxia-inducible factor 1-alpha (HIF1 $\alpha$ ) target genes among others (Kawahara et al., 2009; Zhong et al., 2010).

Compared to other members of the sirtuin family, very little is known about Sirtuin-7 (SIRT7) which is predominantly expressed in the nucleus (Michishita, Park, Bumekis, Barrett, & Horikawa, 2005). It is associated with active rDNA and interacts with RNA polymerase I (Pol I) to stimulate transcription. SIRT7 expression is abundant in the liver, spleen and testes. Conversely its expression is found to be

low in the heart, brain and muscle (Ford et al., 2006). This indirectly correlates SIRT7 with growth as it is mostly found in abundance in highly proliferative tissues.

In short, it has been shown that sirtuins are upstream enzymes which regulate hundreds of downstream enzymes. Table 1.1 lists some of the downstream targets of various sirtuins. By identifying the functions of these proteins and the downstream targets which they regulate, it will be easier in determining which diseases they may be useful in treating.

Table 1.1 Some downstream targets of SIRT1-7.

Downstream targets						
SIRT1	SIRT2	SIRT3	SIRT4	SIRT5	SIRT6	SIRT7
▪ p53	▪ Tubulin	▪ HIF- $\alpha$	▪ PPAR $\alpha$	▪ Nrf2	▪ COX-2	▪ Mir125
▪ NF- $\kappa$ B	▪ p53	▪ Skp2	▪ GLUD1		▪ NF- $\kappa$ B	▪ p53
▪ FOXO	▪ FOXO	▪ p53			▪ HIF- $\alpha$	
▪ BCL6	▪ K-RAS					
▪ CDH1						

#### 1.4 Roles of sirtuins in cancer

The involvement of sirtuins in carcinogenesis cannot be denied as have been demonstrated time and again in the past decade (Saunders & Verdin, 2007; Brooks & Gu, 2008; Lavu, Boss, Elliott, & Lambert, 2008). However, there is yet to be any consensus on the role of sirtuin in cancer owing to the complexity and diversity of their effects. Establishment of the mechanism played by sirtuin in this area remains

obscure. Although research on sirtuin has intensified in the past years, it only revealed the perplexed roles of sirtuins in promoting versus suppressing cancer. Although genes are generally classified as either tumor promoting or tumor suppressing, there are only limited number of genes which fall unambiguously into either one of these categories. The janus-face sirtuins exert their roles depending on different conditions such as the stage of cancer development and other variables which include tissue origin and the cancer microenvironment (Deng, 2009; Bosch-Presegué & Vaquero, 2011; Roth & Chen, 2014).

#### **1.4.1 SIRT1**

SIRT1 remains the most controversial of all sirtuins when it comes to cancer therapy. SIRT1 has been demonstrated to be upregulated in several types of cancer, including colon cancer (Stünkel et al., 2007), prostate cancer (Huffman et al., 2007), pancreatic cancer (Zhao et al., 2011), acute myeloid leukemia (Bradbury et al., 2005) and skin cancer (Hida, Kubo, Murao, & Arase, 2007). In contrast, diminished SIRT1 expression was found in many other cancer types including glioblastoma, bladder carcinoma, ovarian cancer and breast cancer (Wang et al., 2008), highlighting the perplexed role of SIRT1 in cancer.

The capability of SIRT1 as a tumor promoter can be examined across the hallmarks of cancer (Hanahan & Weinberg, 2011). The first evidence of SIRT1 acting as tumor promoter came from experiments showing that SIRT1 deacetylates p53 at its C-terminal Lys382 residue (Vaziri et al., 2001) as loss of p53 tumor suppressor is very common in many cancer types. Apart from p53, there is evidence

of involvement of SIRT1 in epigenetic silencing of tumor suppressor genes and proteins such as secreted frizzled-related protein 1 (SFRP1), cadherin-1 (CDH1), E2F transcription factor 1 (E2F1) and B-cell lymphoma 6 (BCL6) resulting in resistance to cell death (Wang et al., 2006; Pruitt et al., 2006).

Another key tumor suppressor family that is deacetylated by SIRT1 is the FOXO family of transcription factors (Brunet et al., 2004; Daitoku et al., 2004). One of the functions of the FOXO family of genes is their involvement in cell cycle control as well as DNA damage repair (Ho, Myatt, & Lam, 2008; Dansen & Burgering, 2008). Furthermore, SIRT1 deacetylation of FOXO3a has been reported to suppress FOXO3-mediated cell apoptosis which contributed to the promotion of cancer (Motta et al., 2004).

Epithelial-mesenchymal-transition (EMT) which is a key step in morphogenesis is an essential factor in cancer metastasis. SIRT1 has been found to be a regulator of EMT in prostate (Byles et al., 2012) and gastric cancers (Zhang et al., 2013). In enabling replicative immortality through EMT, SIRT1 has been shown to deacetylate HIF (Eades et al., 2011; Dioum et al., 2009) in hypoxic environment, thereby enhancing glucose uptake and tumor cell survival.

On the contrary, SIRT1 plays a role as tumor suppressor by maintaining genetic stability through chromatin regulation and DNA repair (Byles et al., 2010). An elegant study of SIRT1 overexpression in transgenic mice showed that increased SIRT1 expression by three-fold significantly improved healthy mouse aging (Fan & Luo, 2010). The data also showed that mice with upregulated SIRT1 expression

exhibit a reduction in carcinomas and sarcomas. Furthermore, in a liver cancer model, SIRT1 transgenic mice were less susceptible to liver cancer and showed greater protection from both DNA and metabolic damage relative to wild-type mice (Fan & Luo, 2010).

In addition to genetic stability, SIRT1 may regulate other downstream genes via various pathways which contribute to its tumor suppressing function. SIRT1 has been shown to bind to NF- $\kappa$ B which is known to promote cell survival (Wang, Liu, Wang, & Zhang, 2009). SIRT1 deacetylates the p65/Rel-A subunit of NF- $\kappa$ B, thus inhibiting some related anti-apoptotic target genes such as cellular inhibitor of apoptosis-2 (cIAP-2) and B-Cell lymphoma-extra large (BCL-xL) (Yeung et al., 2004). In line with its tumor suppressing function, SIRT1 acts on Breast cancer gene 1 (BRCA1) to negatively regulate another anti-apoptotic gene, Survivin (Wang et al., 2008). Furthermore, SIRT1 targeted and deacetylated H3K9 which promotes Survivin. Therefore, reduction of SIRT1 resulted in elevated Survivin levels and enhanced tumor growth. SIRT1 has also been identified as a tumor suppressor in oral cancer as Chen et al. (2014) showed the overexpression of SIRT1 blocked migration of Oral Squamous Cell Carcinoma (OSCC) cells *in vitro* by targeting Smad4 gene.

#### **1.4.2 SIRT2**

Similar to SIRT1, SIRT2 has both roles in tumor promotion and suppression. SIRT2 was reported to be a tumor suppressor in gliomas (Hiratsuka et al., 2003) and melanomas (Lennerz et al., 2005) while found to be overexpressed in acute myeloid leukemia (Dan et al., 2012) and hepatocarcinomas (Xie, Jung, & Nam, 2011).

Most studies have linked the role of SIRT2 as a tumor suppressor to its mitotic checkpoint function (Dryden et al., 2003). SIRT2 was reported to prevent cells from progressing into mitosis in the presence of microtubule poisons, potentially through the regulation of chromatin condensation (Inoue, Hiratsuka, Osaki, & Oshimura, 2007).

A study by Kim et al. (2011) showed that SIRT2-deficient mice are more susceptible to tumor development due to abnormal chromosomal segregation. A reduction of SIRT2 mRNA expression was also reported in breast cancer and hepatocellular carcinoma (HCC) (Kim et al., 2011). Another recent study by Nguyen, Lee, Lorang-Leins, Trepel, & Smart (2014) showed that SIRT2 interacts with  $\beta$ -catenin to inhibit Wnt signaling. In SIRT2 deficient MEFs, an up-regulation of matrix metalloproteinase 9 (MMP9) and decreased CDH1 expression was observed, leading to increase cell migration and invasion (Nguyen et al., 2014). These indirectly suggest a promotion of cancer metastasis.

Conversely, the capability of SIRT2 to promote cancer can be seen through many, if not all hallmarks of cancer. Similar to SIRT1, SIRT2 deacetylates and downregulate p53 tumor suppressor (van Leeuwen et al., 2013) and K-RAS gene (Yang et al., 2013) to evade growth suppressors and to promote cell survival in response to genotoxic stress (Li et al., 2011). Wang et al. (2012) showed that deacetylation of FOXO3 by SIRT1/SIRT2 results in its degradation, thereby contributing to the promotion of cancer.

Altogether, these data suggested both tumor promoter and suppressor role for SIRT1 and SIRT2. It seems very likely that under normal circumstances, SIRT1/SIRT2 may promote cell survival via DNA repair or inhibition of apoptosis. This in turn suppresses tumorigenesis. However, when the level of cell damage crosses a certain threshold, tumor cells co-opt with SIRT1/SIRT2-regulated pathways to promote cell proliferation and resist apoptosis (Figure 1.4). As such, the role of SIRT1/SIRT2 in cancer is very much dependent on cellular and molecular contexts. This scenario could very much be applied to other sirtuins which have both tumor promoter and tumor suppressor activities.

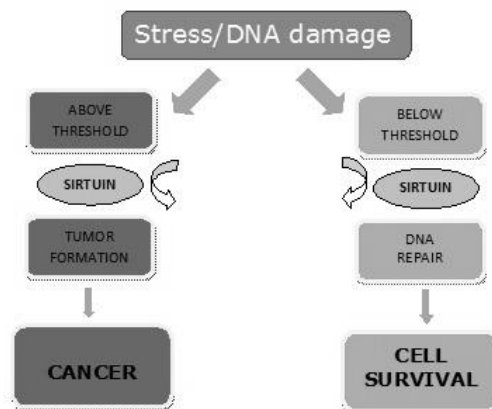


Figure 1.4 Dual role of sirtuin in cancer. Below the stress threshold, sirtuin promotes DNA repair and ultimately cell survival. Above chronic stress threshold, sirtuin induces tumor formation and cancer.

### 1.4.3 SIRT3

Similar to SIRT1 and SIRT2, SIRT3 displays a dual function role in cancer. Under normal conditions it acts as a tumor suppressor and promotes apoptosis (Allison & Milner, 2007; Sundaresan, Samant, Pillai, Rajamohan, & Gupta, 2008)

whereas under stress conditions or DNA damage, it seems to act as a tumor promoter. Low levels of endogenous SIRT3 expression have been reported in breast cancer (Kim et al., 2010). Its role as tumor suppressor was first evidenced through the promotion of mammary tumor formation in SIRT3 knockdown mice (Kim et al., 2010). Consistently, Bell, Emerling, Ricoult and Guarante (2011) later demonstrated that knockdown of SIRT3 in both osteosarcoma and colon cancer resulted in increased tumor size. It was demonstrated that one major tumor suppression mechanism of SIRT3 was through the modulation of Reactive Oxygen Species (ROS) (Finley et al., 2011). Elevation in ROS has been reported to stabilize HIF- $\alpha$ . It thereby contributed positively to tumorigenesis by increasing the expression of HIF-dependent genes such as Vascular Endothelial Growth Factor (VEGF) and phosphoglycerate kinase-1 (PGK-1) (Bell, Emerling, Ricoult, & Guarente, 2011; Schumacker, 2011).

Recently, Inuzuka et al. (2012) discovered a novel tumor suppressor function for SIRT3 through deacetylation of Skp2. Skp2 functions as an E3 ubiquitin ligase and it was shown to target tumor suppressors such as p21, p27 and E-cadherin (Frescas & Pegano, 2008; Tiwari, Ghedolf, Tatari, & Christofori, 2012). Deacetylation of Skp2 by SIRT3 prevents Skp2 from targeting these tumor suppressors and subsequently subdues tumorigenesis. E-cadherin is often linked to EMT and metastasis and its reduction has been observed in many cancer types (Tiwari et al., 2012). Very recently, Huang et al. (2014) also found a tumor suppressive role for SIRT3 in gastric cancer.

Conversely, there is mounting evidence that mitochondrial SIRT3 acts as a tumor promoter. SIRT3 was found overexpressed in several human oral cancer cells (Alhazzazi et al., 2011). Downregulation of SIRT3 in these cells inhibited OSCC cell growth and enhanced the effect of chemotherapeutic drugs. In addition, SIRT3 downregulation in OSCC cells *in vivo* resulted in reduced tumor size in mice, further confirming the role of SIRT3 as a tumor promoter in oral cancer (Alhazzazi et al., 2011). SIRT3 overexpression was also able to rescue p53-induced cell growth arrest in bladder cancer (Li et al., 2010). SIRT3 was found to complex with p53 during the initial stages of its expression. This suggests that SIRT3 may partially reduce the activity of p53 to enact growth arrest and senescence. Taken together, these findings provide some evidence that SIRT3 may have a cell-protective role under stress to promote cancer cell growth.

#### **1.4.4 SIRT4**

Recent advances have shed some light on the roles of SIRT4 in cancer. Many studies have pointed towards SIRT4 as a tumour suppressor. Jeong et al. (2013) first reported the tumor suppressive role for SIRT4 through the inhibition of mitochondrial glutamine metabolism. Their data showed that the deletion of SIRT4 increased glutamine-dependent proliferation and stress-induced genomic instability, resulting in tumorigenesis. Moreover, SIRT4 knockout mice spontaneously develop lung tumors. In continuation of their studies, the authors reported that due to the inhibition of mitochondrial glutamine metabolism by SIRT4, MYC-induced B cell lymphomagenesis was repressed (Jeong et al., 2013). Consistently, Csibi et al. (2013) reported that expression of SIRT4 in cells with activated mechanistic Target

OfRapamycin Complex 1 (mTORC1) repressed the glutamine anaplerosis process and blocked the growth of cells. It was also found that overexpression of SIRT4 in MEFs lacking both TSC2 and p53 had reduced tumor proliferation (Csibi et al., 2013). These studies, albeit few, pointed to a tumor suppressive role for SIRT4.

#### **1.4.5 SIRT5**

Though not yet extensively characterized, some studies have recently linked SIRT5 to cancer. SIRT5 was found to promote cancer growth and facilitate drug resistance in non-small cell lung cancer (Lu, Zuo, Feng, & Zhang, 2014). In the process, Nuclear factor erythroid 2-related factor (Nrf2), a core transcription factor for lung cancer growth and drug resistance, was identified as a target of SIRT5. Due to the scarcity of reports in this area, there is a need for further research to better understand the role of SIRT5 in tumorigenesis.

#### **1.4.6 SIRT6**

As for SIRT6, most current evidence suggests that it acts as a tumor suppressor, considering its function in maintaining genome stability. SIRT6 is frequently deleted or significantly reduced in numerous tumors such as pancreatic and colorectal tumors (Van Meter, Mao, Gorbunova, & Seluanov, 2011). It was found that induction of SIRT6 overexpression in a variety of cancer cell lines resulted in massive apoptosis (Sebastian et al., 2012). Knockdown of SIRT6 resulted in increased tumor incidence in colon cancer model as shown by Sebastian et al. (2012). This was mediated through the reduction of MYC activity and activation of

glycolysis. However, the tumor suppressor role of SIRT6 has been challenged with a recent finding by Ming et al. (2014). They found that SIRT6 promotes COX-2 expression and acts as an oncogene in skin cancer.

#### **1.4.7 SIRT7**

SIRT7 level is elevated in several cancer types such as thyroid (de Nigris et al., 2002), breast (Ashraf et al., 2006), liver (Kim et al., 2012) and colon (Yu et al., 2014) cancer. Substrate for SIRT7 includes mir-125 (Kim et al., 2012) and p53 (Vakhrusheva et al., 2008) among others. Although there is limited information which links SIRT7 to cancer, it is the only sirtuin to date where all current studies points to a tumor promoting role.

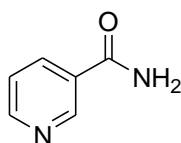
### **1.5 Different classes of sirtuin inhibitors**

Sirtuins first gained prominence when it was reported that their activation might be related to longevity (Kaeberlein, McVey, & Guarente L., 1999; Ghosh, 2008). However, there have since been conflicting views on that matter and the attention has been shifted to sirtuin inhibitors as they have been linked to the pathogenesis of cancer (Martinez-Pastor, & Mostoslavsky, 2012). Although sirtuin overexpression might be beneficial in preventing cancers, sirtuin activators (especially SIRT1 activators) are seldom touted as potential anti-cancer agents. In fact, most if not all of the small molecule sirtuin modulators which showed anti-cancer properties are inhibitors.

In the past, the development of sirtuin inhibitors was focused mainly on SIRT1–3. This was mainly due to the limited possibilities in determining the inhibitory activity against SIRT4–7 using the enzymatic assays as they only show weak or no deacetylation activity to known protein substrates. However, the discovery of enzymatic activities other than deacetylation for SIRT5 and SIRT6 and the expanding list of known protein targets for SIRT4–7 enable now the development of inhibitors for these isoforms. However, as SIRT1 and SIRT2 remain two of the best characterized sirtuins, most sirtuin inhibitors developed currently are targeted towards these two isoforms.

### **1.5.1 Nicotinamide derivatives**

Nicotinamide (Figure 1.5), which is a physiological inhibitor of Sir2, was shown to inhibit SIRT1 and SIRT2 with  $IC_{50}$  values of approximately 50  $\mu$ M and 100  $\mu$ M respectively (Tervo et al., 2004). Initial studies reported nicotinamide to be a non-competitive inhibitor of SIRT1 and SIRT2 that interacts with the C-pocket (nicotinamide pocket) in the binding site (Bitterman, Anderson, Cohen, Latorre-Esteves, & Sinclair, 2002). However, later discoveries suggest that the probable interaction could be due to reverse reaction of nicotinamide with *O*-alkylamidate I (Sauve, Wolberger, Schramm, & Boeke, 2006). There could, however, be limited potential to inhibitors of this class as further modifications to nicotinamide aimed to increase the potency against SIRT1/SIRT2 inhibition proved unsuccessful (Jackson, Schmidt, Oppenheimer, & Denu, 2003; Schmidt, Smith, Jackson, & Denu, 2004).



**Nicotinamide**

Figure 1.5 Structure of nicotinamide

### 1.5.2 Suramin and its analogs

Suramin (Figure 1.6) is a symmetric polyanionic naphthylurea. It was discovered to have sirtuin inhibitory activity during a screening for SIRT1 activators (Howitx et al., 2003). It is a potent SIRT1 inhibitor with IC<sub>50</sub> value of 0.3  $\mu$ M (Trapp et al., 2007). By replacing the central symmetrical bis(*meta*-carboxyphenyl)urea moiety by an isophthalic acid, Trapp et al. (2007) have exploited the suramin backbone and managed to identify a selective SIRT1 inhibitor (NF675, Figure 1.6) with IC<sub>50</sub> value of 0.1  $\mu$ M. However, the use of suramin as potent sirtuin inhibitor and future therapeutic application was set back by its nephrotoxicity (Figg et al., 1994) and neurotoxicity at high concentration (Gill, Hobday, & Windebank, 1995).

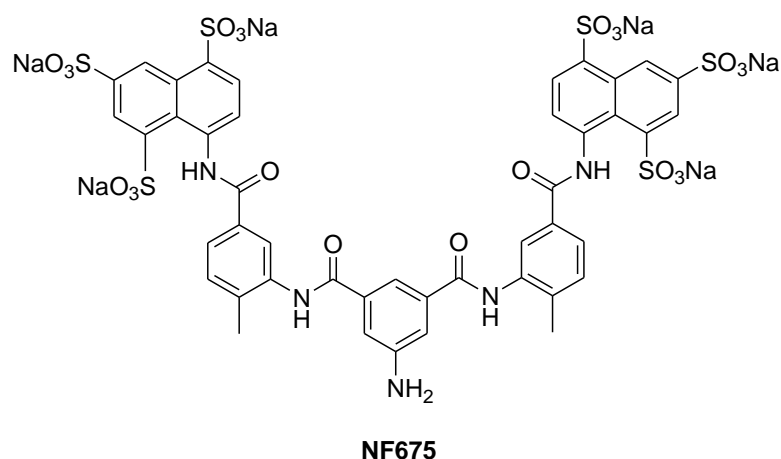
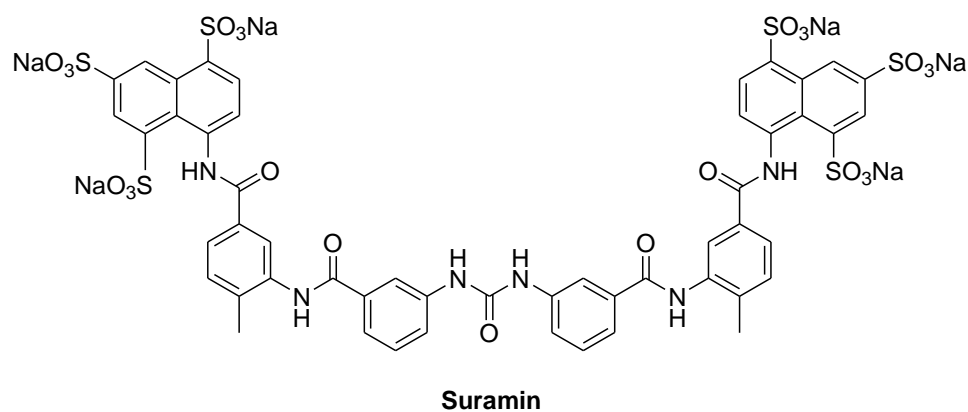


Figure 1.6 Structure of Suramin and NF675.

### 1.5.3 Splitomicin and its analogs

Splitomicin (Figure 1.7) was discovered to inhibit Sir2p and HST1 in micromolar level in a cell-based screen (Bedalov, Gatbonton, Irvine, Gottschling, & Simon, 2001). As this molecule is small (molecular mass < 200), it represents an attractive lead model for histone deacetylase inhibitors such as sirtuins. It was found that different structural changes to the splitomicin scaffold accounted for inhibitor selectivity (Hirao et al., 2003). Based on the knowledge gathered earlier, more potent inhibitors of human subtypes were later developed. An alpha-phenyl splitomicin with a bromo-substituent in 8-position coded HR73 (Figure 1.7) was found to inhibit

SIRT1 with an  $IC_{50}$  value of 5  $\mu M$  and it was shown to decrease HIV transcription via acetylation of Tat protein (Pagans et al., 2005). Similarly, Neugebauer and co-workers also screened a number of splitomicin analogs and they too managed to identify SIRT2 selective inhibitors in the low micromolar range (Neugebauer et al., 2008). Through this work, the acetyllysine pocket was identified as the binding site for splitomicin and SIR2p. Nevertheless, it was noted that splitomicin and its analogs did not show potent anti proliferative activities towards MCF-7 breast cancer cells (Neugebauer et al., 2008). More recent splitomicin derivatives are also not potential therapeutic leads as they consist of metabolically unstable groups and are generally very lipophilic in nature (Freitag et al., 2011).

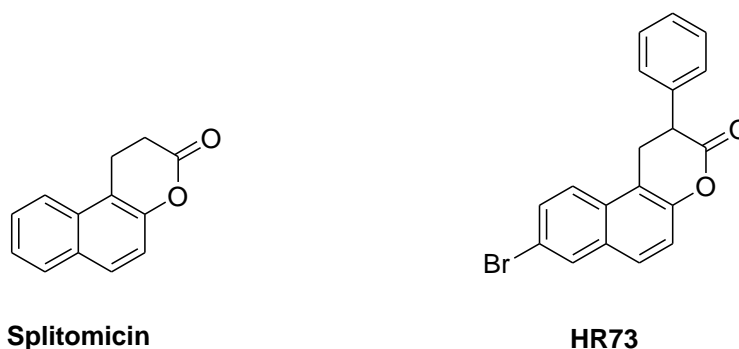


Figure 1.7 Structure of Splitomicin and HR73.

#### 1.5.4 Hydroxynaphthaldehyde derivatives

Certain compounds bearing the hydroxynaphthaldehyde scaffold have been found to possess sirtuin inhibitory activities. Sirtinol (Figure 1.8), one of the first synthetic sirtuin inhibitors, was identified during a high-throughput phenotype screening for yeast SIR2 inhibitor (Grozinger, Chao, Blackwell, Moazed, & Schreiber 2001). It showed an  $IC_{50}$  of 68  $\mu M$  for yeast SIR2p. It was further evaluated for human sirtuin inhibitory activities and is now considered a non-



Another sirtuin inhibitor with hydroxynaphthaldehyde moiety is cambinol (Figure 1.9). It is a pan SIRT1/SIRT2 inhibitor with IC<sub>50</sub> values of 56 μM and 59 μM for SIRT1 and SIRT2 respectively (Heltweg et al., 2006). Although the *in vitro* investigation did not point to an extremely potent sirtuin inhibitory activity, it was nevertheless a strong lead compound as treatment of BCL6-expressing Burkitt lymphoma cells with cambinol led to apoptosis *in vivo* and also in mouse xenograft model. Due to its potential, various derivatives of cambinol have been designed, synthesized and evaluated in the search for more potent sirtuin inhibitors. More recent works have reported cambinol derivatives having IC<sub>50</sub> values in the low micromolar range (Medda et al., 2009; Medda et al., 2011). Furthermore, recent optimization of cambinol structure has resulted in the identification of pyrazolone and isoxazol-5-one based analogues (coded **8**, **17** and **24**) which are isoform selective sirtuin inhibitors (Figure 1.9) (Mahajan et al., 2014).



**Cambinol**

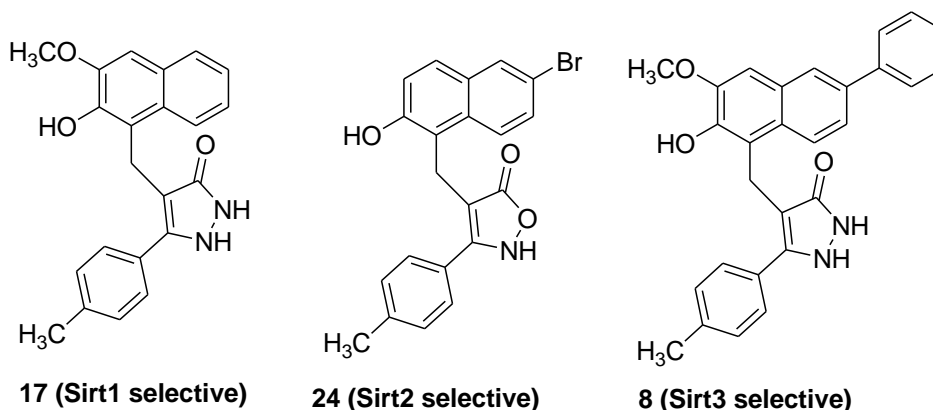


Figure 1.9 Structure of cambinol and other sirtuin inhibitors with the hydroxynaphthaldehyde moiety.

### 1.5.5 Thiobarbiturates derivatives

Thiobarbiturates are structurally related to cambinol, with thiourea moiety an integral part of their structure. The first seven active inhibitors of this scaffold were uncovered in a virtual screening of over 300,000 compounds in Chembridge database (Uciechowska et al., 2008). Through molecular docking, these compounds were postulated to interact with the nicotinamide binding pocket analogous to cambinol. These compounds are generally unselective with regards to SIRT1 and SIRT2 with inhibition potency in micromolar levels (Uciechowska et al., 2008). Based on the molecular simulation data generated, several novel thiobarbiturates were synthesized, some of them showing SIRT1/SIRT2 selectivity based on different substituents attached to the thiourea substructure (Uciechowska et al., 2008).

### 1.5.6 Indole derivatives

Among the most potent and selective SIRT1 inhibitor identified to date is EX-527 (Figure 1.10), which is based on the indole structure. It was discovered during a fluorescent-based high-throughput screening by Napper et al. (2005). EX-527 showed remarkable SIRT1 inhibition potency with  $IC_{50}$  value of 100 nM. Evaluation of its stereochemistry through kinetic studies as well as crystal analysis revealed that the (S)-enantiomer is the active isomer (Zhao et al., 2013). Furthermore, refined crystal analysis by Gertz et al. (2014) indicated that EX-527 requires  $NAD^+$  for its inhibition activity and it occupies the nicotinamide binding site in SIRT1. EX-527 was found to increase the acetylation level of p53 but has no effect on cell survival after DNA damage (Solomon et al., 2006). It also failed to induce cell death in a separate study (Peck et al., 2010).